A two-dimensional electromagnetic vibration energy harvester with variable stiffness

Imbaquingo, Carlos; Bahl, Christian; Insinga, Andrea R.; Bjørk, Rasmus

Published in:
Applied Energy

Link to article, DOI:
10.1016/j.apenergy.2022.119650

Publication date:
2022

Document Version
Publisher's PDF, also known as Version of record

Applied Energy 325 (2022) 119650

Contents lists available at ScienceDirect

Applied Energy

journal homepage: www.elsevier.com/locate/apenergy

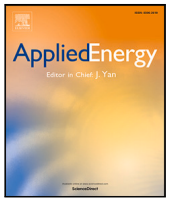

A two-dimensional electromagnetic vibration energy harvester with variable stiffness

Carlos Imbaquingo *, Christian Bahl, Andrea R. Insinga, Rasmus Bjørk

Department of Energy Conversion and Storage, DTU Energy, Kongens Lyngby, 2800, Denmark

ARTICLE INFO

Keywords:
Electromagnetic energy harvester
2D electromagnetic harvester
Two-dimensional vibration
Variable stiffness
Magnetic stiffness

ABSTRACT

This work investigates the performance of an electromagnetic vibration harvester for two-dimensional vibrations with variable magnetic stiffness and electromagnetic damping. The device consists of a free-to-move cylindrical magnetic structure with a set of bearings located on top and bottom, a couple of coils located on top and bottom of the device and finally a fixed system of disk-shaped magnets placed inside a ring holder. The number of disk-shaped magnets in the ring holder can be varied to change the magnetic stiffness of the system. The performance of the device is characterized experimentally for nine different configurations of disk-shaped magnets, exploring both symmetric and asymmetric designs. Using an XY-shaker to vibrate the system in two dimensions in frequencies from 1 Hz to 10 Hz and with motion amplitude of 2 mm on both axes, a maximum power of 27 mW was harvested. This occurs for an asymmetric device, i.e. with different magnetic stiffnesses along its two axis. For symmetric devices the power is lower by a factor of two. Finally, varying the electromagnetic damping, which is controlled by varying the coil dimensions, can further increase the power to 42 mW.

1. Introduction

Harvesting energy to power sensors for both wearable and Internet-of-Things (IoT) devices is a topic with a steep increasing interest [1–3]. Such energy harvesters can replace batteries in sensor devices and thereby save both the time and cost associated with replacing the batteries when these wear out, at the same time reducing the environmental issues with using batteries in the first place [4].

Energy can be harvested from the environment through a number of different sources. Here vibration energy harvesting is considered since it has the benefit of working both indoors and outdoors and in both cold and warm environments. It is also ideally suited for wearable devices, where the vibrations from human motion can directly be harvested [5]. Harvesting vibrational energy can be done through three approaches, namely piezoelectric, electrostatic and electromagnetic techniques. This study focuses on the latter type of harvester, as there is great flexibility in the design of such devices [6].

Electromagnetic vibration energy harvesters (EMVEH) are typically designed to fit their exact application, i.e. the harvester is tuned to resonate at a very specific frequency already in the design phase. This limits the power that can be harvested to a narrow range around exactly this resonant frequency [7,8]. A conventional EMVEH consists of three co-axial magnets arranged with opposing polarities, such that the middle magnet is floating and free to move relative to a set of coils [9–12] although other types of designs exists [13–16]. The power produced by a centimeter-sized device is typically in the μW-mW range [17]. EMVEHs are usually designed to vibrate only along one direction [17] with the inherent limitations of device design and functionality that this results in [18].

To overcome these limitations EMVEHs that can vibrate in multiple directions have been considered. Recently, a novel elliptically shaped EMVEH for two-dimensional motion was studied, which allowed for a wider bandwidth than traditional 1D harvesters [19]. This 2D-EMVEH consisted of a free-to-move ring-shaped permanent magnet with radial magnetization and ball-bearings on the top and bottom, a fixed system of square magnets placed inside an elliptically shaped holder, and coils located above and below the harvester. Unlike 1-D harvesters, the resulting output power showed two resonant frequencies at which the harvester generated around 1.5 mW. However, this device did not have any variable properties and no investigation was done on how to optimize power production, but the device merely experimentally showed that 2D motion can be harvested. A somewhat similar structure as discussed above, i.e. where the moving part is the middle magnet and also with coils placed on the outside of the design has been considered previously [20] but here the configuration was used only to decrease friction and not for scavenging energy from two-dimensional vibrations. Likewise, Ref. [21] considered a spherical permanent magnet

* Corresponding author.
E-mail addresses: ceim@dtu.dk (C. Imbaquingo), chrb@dtu.dk (C. Bahl), aroin@dtu.dk (A.R. Insinga), rabj@dtu.dk (R. Bjørk).

https://doi.org/10.1016/j.apenergy.2022.119650
Received 22 December 2021; Received in revised form 17 June 2022; Accepted 7 July 2022
Available online 17 August 2022

inside a capsule which is wound with two coils. Due to the lack of a repulsive force, this prototype needs stoppers on the inner walls of the capsule so that the spherical magnet does not break. Finally, Ref. [22] considered how an eccentric mass brings about an oscillatory motion which, under certain conditions, results in a rotary 2D motion.

The above discussion shows that there is a clear knowledge gap in literature on the dynamics of two-dimensional EMVEHs, especially concerning the optimal harvester design. The influence of the critical system properties, such as magnetic stiffness and electromagnetic damping, on the behavior and output power of the harvesters is not known and existing designs in literature have only explored fixed designs with no variation of the system properties [19–22]. Therefore an investigation on the optimal harvester design with respect to the properties of the system that can be controlled after the design phase of the harvester is clearly warranted. The shape of the harvester cannot be altered once the harvester is produced, but the magnetic stiffness and the electromagnetic damping can. Here we investigate a multi-purpose device where the magnetic stiffness in the device can be altered at will. The hypothesis is that instead of modifying the geometry of the device to adapt it to the vibrational source, the magnetic stiffness in the device can instead be altered to change the resonant frequencies. This will be much more practical for applications as a single device can be used for multiple applications. In the design proposed here, changing the magnetic stiffness is simply done by adding or removing magnets in the outer confining structure of the harvester, thereby changing the magnetic stiffness independently in different directions, and through this obtaining a potentially broadband harvester. We quantify the behavior of such device for a total of nine different symmetric and asymmetric configurations of magnets to understand how to optimize a prototype to a given vibration source.

2. Device

In order to realize a harvester where the magnetic stiffness can be easily controlled, this needs to be highly modular. Hereby, a two-dimensional ring-shaped electromagnetic vibration energy harvester that consists of the three parts depicted in Fig. 1 is studied. The first part is a free-to-move three-cylinder magnetic structure with bearings on top and bottom. The second part encapsulates the moving structure, and consists of a ring holder with 24 holes placed in a circle on the top and bottom faces symmetrically, i.e. with 48 holes in total, where one or two disk-shaped magnets can be placed in each hole. The third part is a pair of coils placed on the top and bottom of the harvester. The dimensions and component specifications of the individual parts are listed in Table 1. A photo of the actual device is shown in Fig. 3.

The disk-shaped magnets placed in the holes of the ring holder are tilted 45°, so that they create a magnetic flux line distribution as illustrated in Fig. 2. This brings about a spring-like restoring force that pushes back the moving structure when it is affected by an external vibration source, resulting in a variable magnetic flux seen by the fixed coils, inducing an EMF in these. The magnetic stiffness of the device can be changed by changing the number of disk-shaped magnets in each hole, which can contain one or two disk-shaped magnets. The first magnet in each hole is glued in place. Inserting a second magnet is easy, as the magnetic force pulls it inwards. Removing it can also be done fairly easily as the slated holes allow for a prying tool to be inserted between the magnets in each hole, so that they can be separated and one of them removed. When two magnets are in a hole, they simply act as a twice-as-long magnet compared to a single magnet.

To ensure that the free-to-move structure of three cylindrical magnets does not flip over in accordance with Earnshaw's theorem, two plates are placed just below and above this to confine the movement plane to two dimensions. Additionally, polymer ball transfer bearings (BB-505-B180-POM from Igus) are placed on the free-to-move cylindrical structure to help decrease any friction between the moving structure and the plates.

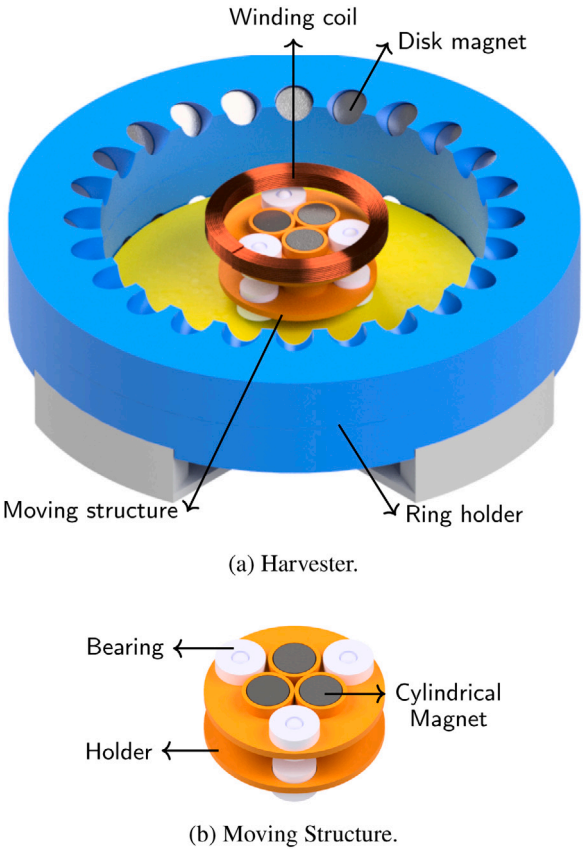

Fig. 1. (a) Schematic of the 2D electromagnetic energy harvester. A 300-turn coil is shown on top. The inner diameter of the ring holder is 105 mm. There are disk-shaped magnets both above and below the plane of movement of the cylindrical magnets, although only the disk-shaped magnets above the plane can be seen. Only the confining plate below the moving structure is shown (in yellow). (b) The moving structure with three cylindrical magnets and six polymer ball bearings.

Table 1
Dimensions and component specifications.

Component	Parameter	Quantity
Cylindrical Magnets	Amount	3
	Diameter	10 mm
	Height	20 mm
	Grade	NdFeB, N45
Disk Magnets	Amount	Varying
	Diameter	10 mm
	Height	5 mm
	Grade	NdFeB, N52
Coil Windings	Inner diameter	27 mm
	Outer diameter	40 mm
	Height	2.5 mm
	Number of turns	300
	Wire gauge	0.202 mm
	Resistance	16.5 Ω
	Inductance	3.77 mH
Ring Holder	Inner diameter	105 mm
	Outer diameter	154 mm
	Height	30 mm

Two 300-turn coils are glued to the top and bottom plates of the harvester, and their inner diameter is similar to the outer diameter of the free-to-move structure of the cylindrical magnets as can be seen in Fig. 3. The two coils are connected in series to get the sum of the two EMF signals, and the connected load matches with the internal resistance of the coils to attain maximum transfer power [23]. The low impedance due to the internal inductance of the coils is neglected. This

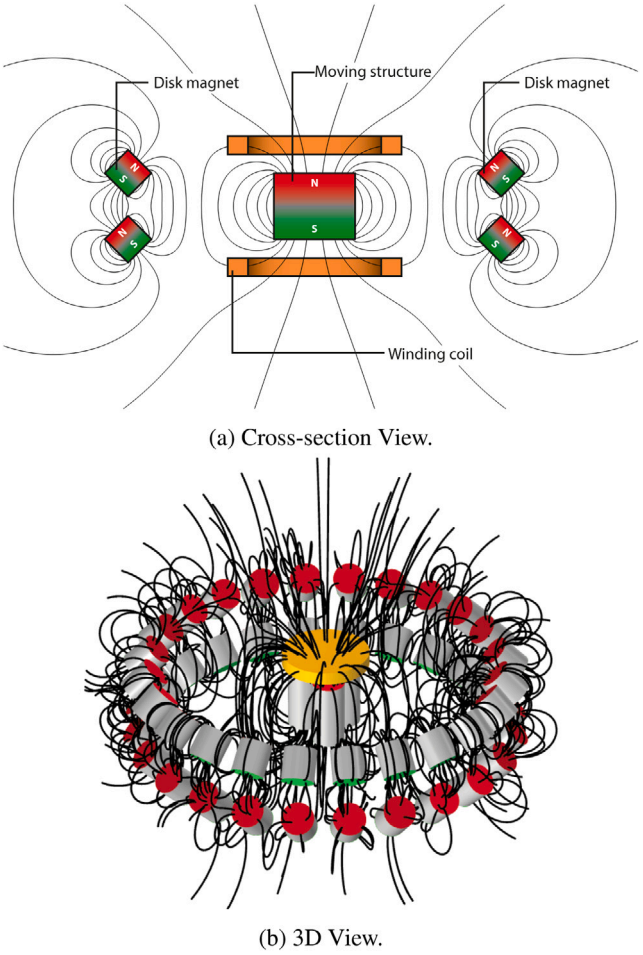

Fig. 2. (a) Cross-section of the 2D EMVEH and magnetic flux lines between the disk-shaped magnets in the ring holder (left and right) and the free-to-move structure (center) consisting of three cylindrical magnets, although this cross-section only shows one magnet for brevity and (b) the field lines shown in 3D as calculated using the finite element framework Comsol. As in (a) the color indicates the magnetic pole.

is justified as e.g. at 10 Hz the impedance is 0.24 Ω which is much lower than the internal resistance of the coils.

2.1. Physics of the 2D device

The physics and equation of motion of the 2D harvester is identical to that of the well-known 1D electromagnetic harvesters except that the motion is in two dimensions. A 1D electromagnetic harvester has the following equations of motion [8]:

$$m_{\text{free}}\ddot{z} = F_{coil}(z, \dots, I_n, \dots) + F_{mag}(z) + F_g + F_{frict}(\dot{z}) \tag{1}$$

$$L_n\dot{I}_n + \sum_{n'} L_{n,n'}\dot{I}_{n'} + R_n I_n + \dot{z}\frac{d\phi_n}{dz_n} = 0 \tag{2}$$

where z is the position variable, m_{free} is the mass of the free-to-move magnet, F_{coil} is the force due to the interaction of the free-to-move magnet with the coil windings [12,24], F_{mag} is the force due to the interaction of the free-to-move magnet with the fixed magnets, F_g is the gravitational force and $F_{frict} = -c\dot{z}$ is a friction force. The second equation, which determines the electrical condition of a coil winding is stated for the nth coil winding but an equation exists for every independent coil winding. For the nth coil winding a current I_n is running, and where L_n is the self-inductance of each coil, $L_{n,n'}$ is the mutual inductance between the n_{th} and n'_{th} coils, R_n is the resistance connected to each coil winding and ϕ_n is the magnetic flux density

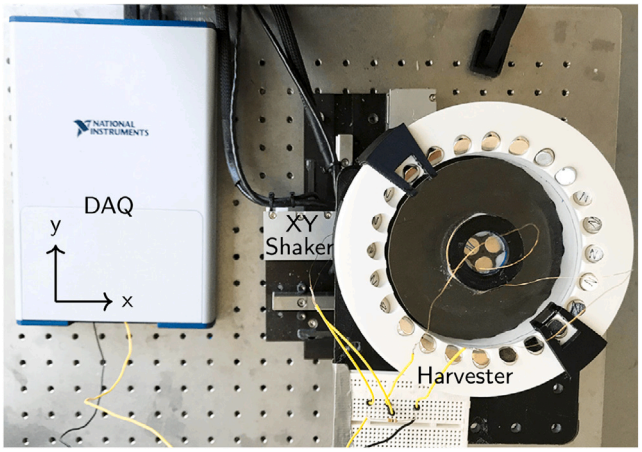

Fig. 3. A top view of the actual prototype in white and the experimental setup. Specifically, it shows the "f"-case described in Table 3.

through the coil winding. If the coil windings are connected in series, the system of equations is simplified as only one current and one resistance is present.

For the harvester considered in this work, the free-to-move structure can move in two dimensions, i.e. in both the x and y directions. Thus the magnetic force depends on both the x and y coordinates and the coil winding force depend on the x and y coordinates as well as the velocities v_x and v_y. For the flux through a coil winding the position variable is the planar distance between the free-to-move structure and the coil winding, r. This planer distance is given as $r = \sqrt{x_{\text{rel}}^2 + y_{\text{rel}}^2}$ with $x_{\text{rel}} = (x_c - x_f)$ and $y_{\text{rel}} = (y_c - y_f)$ where the free-to-move structure has coordinates (x_f, y_f) and the coil winding has coordinates (x_c, y_c). Therefore, the equations of motion for the 2D EMVEH is

$$\begin{aligned} m_{\text{free}}\ddot{x} &= F_{coil,x}(x, y, \dots, I_n, \dots) + F_{mag,x}(x, y) + F_{g,x} + F_{frict,x}(\dot{x}) \\ m_{\text{free}}\ddot{y} &= F_{coil,y}(x, y, \dots, I_n, \dots) + F_{mag,y}(x, y) + F_{g,y} + F_{frict,y}(\dot{y}) \end{aligned} \tag{3}$$

and

$$L_n\dot{I}_n + \sum_{n'} L_{n,n'}\dot{I}_{n'} + R_n I_n + v_{\text{dir}}\|v_\parallel\|\frac{d\phi_n}{dr_n} = 0 \tag{4}$$

Again there is a differential equation for each independent coil winding but only the nth equation is given. Here $v_\parallel$ is the velocity parallel to the planar position vector r connecting the free-to-move structure and the coil winding. The direction v_{dir} indicates if the free-to-move structure is moving towards or away from the coil winding.

The parallel component of the velocity in the x- and y-directions are thus

$$\begin{bmatrix} v_{\parallel,x} \\ v_{\parallel,y} \end{bmatrix} = \frac{v_x x_{\text{rel}} + v_y y_{\text{rel}}}{x_{\text{rel}}^2 + y_{\text{rel}}^2}\begin{bmatrix} x_{\text{rel}} \\ y_{\text{rel}} \end{bmatrix} \tag{5}$$

And the direction of the velocity of the free-to-move structure towards or away from the coil winding as given by v_{dir} is

$$v_{dir} = \frac{v_{\parallel,x}x_{\text{rel}} + v_{\parallel,y}y_{\text{rel}}}{|v_{\parallel,x}x_{\text{rel}} + v_{\parallel,y}y_{\text{rel}}|} = \text{sign}\left(v_{\parallel,x}x_{\text{rel}} + v_{\parallel,y}y_{\text{rel}}\right) \tag{6}$$

This will be equal to +1 when the magnet is moving towards the coil winding and to −1 when it is moving away from the coil winding.

The magnetic force can be found using e.g. a finite element framework for a specific device geometry. The coil winding force must consider the relative distance as mentioned above, i,e. the coil winding force on the free-to-move structure from the nth coil winding is given by

$$F_{coil,x,n}(\dot{x}, x, \dot{y}, y, I_n) = I_n\frac{d\phi_n}{dr_n}\frac{x_{\text{rel,n}}}{\sqrt{x_{\text{rel,n}}^2 + y_{\text{rel,n}}^2}} \tag{7}$$

$$F_{coil,y,n}(\dot{x}, x, \dot{y}, y, I_n) = I_n \frac{d\phi_n}{dr_n} \frac{y_{\text{rel,n}}}{\sqrt{x_{\text{rel,n}}^2 + y_{\text{rel,n}}^2}} \tag{8}$$

and the total force is just the sum from all coil windings.

3. Experimental setup

To examine how the 2D EMVEH behaves for different magnetic stiffnesses, i.e. different amount of disk-shaped magnets in the ring holder, the device must be experimentally characterized. This was done by using the experimental setup depicted in Fig. 3, where a two dimensional shaker (SRS-004-006–004-003-01-XY from H2W Technologies) was employed to generate the vibration source. This shaker has two platforms that move perpendicularly to each other, giving as a result a two-dimensional motion that follows Lissajous patterns, i.e. where the movement in the two directions are independently given by a sinusoidal curve. The induced EMF signals of the coils were measured by a USB-6351 data acquisition card from National Instruments with a sample frequency of 1 kHz.

The number of disk magnets in the ring holder determines the strength of the spring-like restoring force, i.e. the magnetic stiffness of the system. To examine and understand the movement and power production of the device with different magnetic stiffness, a set of nine different magnet distributions were tested. These are described in detail in the following. In order to ensure that there is a minimum magnetic stiffness (and therefore restoring force) in the device, each hole in the ring holder has a minimum of one disk-shaped magnet inserted at all times. The top and bottom configurations of disk-shaped magnet in the ring holder are always filled identically.

In all experiments the displacement amplitude of each platform of the XY-shaker was 2 mm, the bottom platform of the XY shaker is aligned with the y-axis of Fig. 3 and its motion has a constant frequency of 4 Hz. The top platform is aligned with the x-axis and its motion frequency was varied from 1 Hz to 10 Hz in steps of 0.25 Hz, and in steps 0.05 Hz around the resonance frequency, starting from rest for each frequency. These frequencies are chosen because the dominant step frequency of human walking falls at around 2–3 Hz [5]. However, due to the inherently inverse relationship between resonant frequency and harvester size, obtaining a resonant frequency in the 2–3 Hz range would require an obtrusively large harvester, excluding it from wearable electronics applications. For this reason, wearable energy harvesters are designed to have a resonant frequency matching one of the higher harmonics of the dominant step frequencies, around 6–8 Hz [5]. Energy from human motion has previously been harvested by electromagnetic energy harvesters [10,25–31]. However, this is just one of many potential applications, including vibrating structures, animal movement or transport applications. Especially applications where the moving object to which the harvester is attached has a potential two-dimensional motion would be beneficial. This could for example be around the collar of an animal, where the movement is both up and down due to the animal gait and left and right due to head movement sideways.

4. Results

In each experiment the combined voltage in the coils was recorded for a period of 3 s after the system reached steady state. Fig. 4 shows the output voltage as function of time for an experiment with frequencies of 7.7 Hz and 4 Hz in the x- and y-directions, respectively. As it can be seen from the figure, the voltage displays a steady-state behavior with a period of around 65.5 ms for this given set of frequencies and amplitudes.

As previously mentioned, the internal coil inductance is neglected due to the low impedance. Therefore, the load resistance R_L connected to the harvester matches the total internal resistance of the two coils, and the output power P_o is calculated with Eq. (9),

$$P_o = \frac{V_{rms}^2}{R_L}, \tag{9}$$

where V_{rms} is the root-mean-square voltage over the connected load R_L.

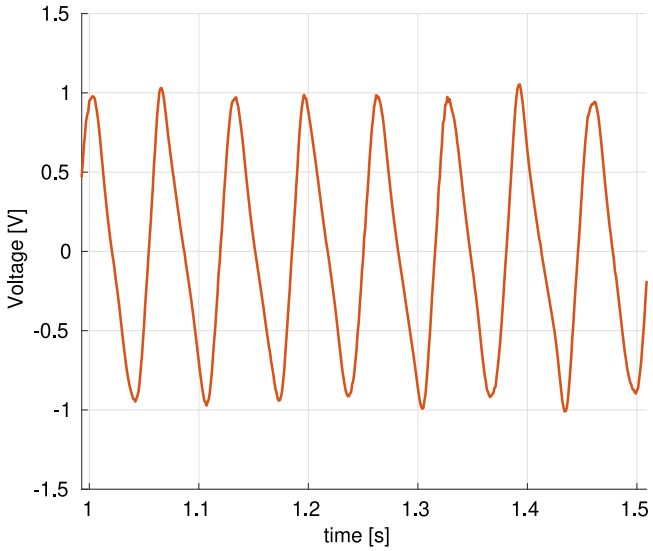

Fig. 4. Output voltage of configuration "c" of Table 2 with frequencies of 7.7 Hz and 4 Hz on the x and y axes respectively and amplitude of 2 mm on both axes.

4.1. Symmetric magnetic stiffness

First, increasing the magnetic stiffness symmetrically is explored, i.e. in such a way that the ring-shaped holder is as magnetically symmetric as possible in the xy-plane. Hence, four different arrangements of magnets in the ring holder are considered, as illustrated in Table 2. The magnetic stiffness is increased by placing more disk-shaped magnets in the ring holder successively. The power as measured experimentally for the different configurations are shown in Fig. 5. It is immediately apparent that for case "a" there is a low output power, which is because the amount of magnets is not enough to create a considerable restoring force which can manage to push back the moving structure. As a consequence, the moving structure has almost no relative motion, hence no voltage is induced in the coils. As the number of magnets in the ring holder is increased successively in cases "b", "c" and "d", the magnetic stiffness is increased and thus the moving structure experiences enough restoring force to push it back and forward inducing an EMF in the coils and hence producing output power. It is also clear that the higher the restoring force is, the larger the resonance frequency will be, as could also be expected from the physics of simple harmonic motion. The peak frequency is at 7.3 Hz, 7.7 Hz and 8.2 Hz for the cases "b", "c" and "d", respectively. Normalizing to the "b" peak frequency this gives a ratio of peak frequencies of 1.0:1.055:1.123.

To estimate the magnetic stiffness that each configuration of magnets in Table 2 gives rise to, we use a magnetostatic model in the finite element software Comsol, and calculate the magnetic force in the three cases "b", "c" and "d" on the cylindrical magnets in the moving structure as this is brought closer to the ring holder. The force is calculated from Maxwells stress tensor. This restoring force as function of displacement, r, was then fitted with Hooks law, $F_m = -kr$, in the central part of the system where the force is linear [8]. The determined values for the spring constant, i.e. the magnetic stiffness, k, are 0.16 N/mm, 0.18 N/mm and 0.22 N/mm. The restoring force is shown in Fig. 6 as well as the linear fits. For a simple harmonic oscillator, the frequency scales as $\sqrt{k}$, and thus the frequency ratios, if the system had been a simple harmonic oscillator, would be 1.0:1.061:1.173, which are close to the observed ratios. The discrepancy is caused by the fact that the experimental system is a damped driven nonlinear oscillator.

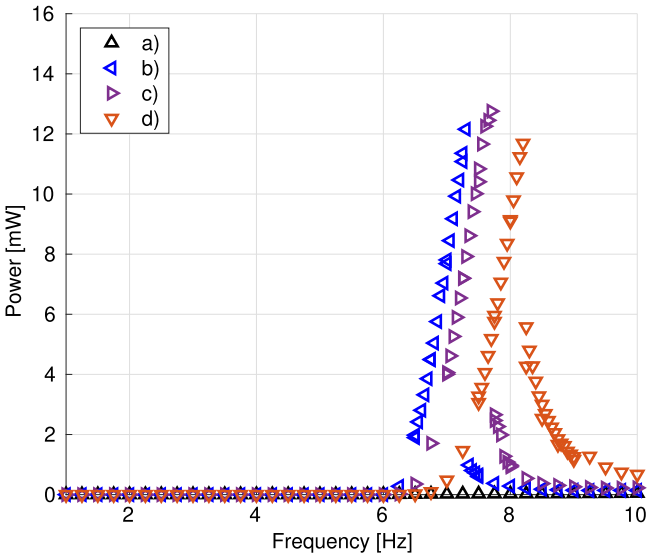

Fig. 5. The power as function of frequency in the x-direction for the device configurations given in Table 2. The y-direction has a fixed frequency of 4 Hz.

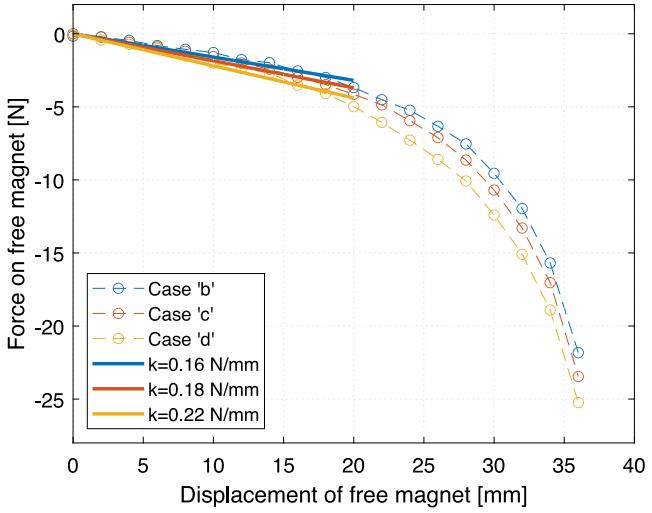

Fig. 6. The restoring force as function of displacement of the free magnets for the cases "b", "c" and "d" as determined using Comsol. The linear fits determining the magnetic stiffness is also shown.

4.2. Two-pole asymmetric magnetic stiffness

Having explored a symmetric increase in magnetic stiffness, the dynamics of the device in asymmetric cases is explored. The disk-shaped magnets are placed such that the magnetic restoring force becomes asymmetric in either the x- or y-direction, as described in Table 3. For example, for case "e" the magnetic stiffness in one direction will be identical to that of case "a", while it will be identical to that of case "d" in the orthogonal direction. The produced power as function of frequency is shown in Fig. 7. It is seen that by adding disk-shaped magnets asymmetrically as described in the "e"-case, the harvester reaches a maximum output power twice as high as that in the previous symmetric case. This is because the resulting magnetic stiffness comes from the concentrated magnetic flux in the x-direction, bringing about a stronger magnet–magnet interaction hence more generated power. However, this implies a higher resonance frequency as seen in Fig. 7. On the contrary, the "f"-case produces almost no power due to the lack of restoring force in the direction where the frequency sweep is performed. Finally the "g"-case shows that by only concentrating the magnetic flux in one side, the resulting power and resonance frequency are comparable to the ones attained in the symmetric magnetic stiffness analysis.

Table 2
The four tested symmetric configurations. The circles around each letter indicate the individual holes in the top face of the ring holder. The bottom face is identical. An empty circle means that the individual hole contains one disk-shaped magnet, while a green filled circle indicate that the hole contains two disk-shaped magnets.

a	The base configuration with one disk-shaped magnet in each hole in each ring holder
b	The ring holder has 72 magnets, with two disk-shaped magnets in every second hole and one magnet in every other hole.
c	The ring holder has 80 magnets, with two disk-shaped magnets in two consecutive holes and the next hole only having one disk-shaped magnet.
d	Two magnets in each hole, giving a total of 96 magnets in the ring holder.

Table 3
The three tested two-pole asymmetric configurations in a style similar to Table 2. The direction in which the frequency of the vibration source has been varied has been indicated.

e	The ring holder has 76 magnets. There are 7 holes with two disk-shaped magnets on each side of the harvester and two "gaps" of 5 holes with just one disk-shaped magnet. The frequency is swept in the direction with two magnets in each hole.
f	Identical to the previous configuration, "e", except rotated by 90°.
g	The ring holder has 66 magnets, with 9 holes with two disk-shaped magnets on one side of the device. The frequency is swept in the direction similar to "e".

Table 4
The two tested three-pole asymmetric configurations in a style similar to Table 2.

h	The ring holder has 66 magnets, with a triangular configuration of sets of three consecutive two disk-shaped magnets.
i	Same triangle configuration as the previous configuration, "h", but with 5 consecutive two disk-shaped magnets at each vertex, giving a total of 78 magnets in the ring holder.

4.3. Three-pole asymmetric magnetic stiffness

Having seen that a two-pole asymmetric device can produce a substantial increase in power production, a further increase in pole number could result in an even higher power production. Therefore, the disk-shaped magnets in the ring holder are placed in a triangular pole distributions as detailed in Table 4. The results from the experimental characterization of the device are shown in Fig. 8. It can be seen that increasing the magnetic stiffness, i.e. going from the "h"-case to the "i"-case, slightly increases the resonance frequency as was also seen for the symmetric cases. However, here the output power also increases noticeably, which was not the case for the symmetric devices. Overall the produced power is lower than for the two-pole case and is comparable to the symmetric cases. This is most likely because these devices have a higher order symmetry (three-pole) than the vibrational directions (two directions), which causes them to behave as if they were fully symmetric devices.

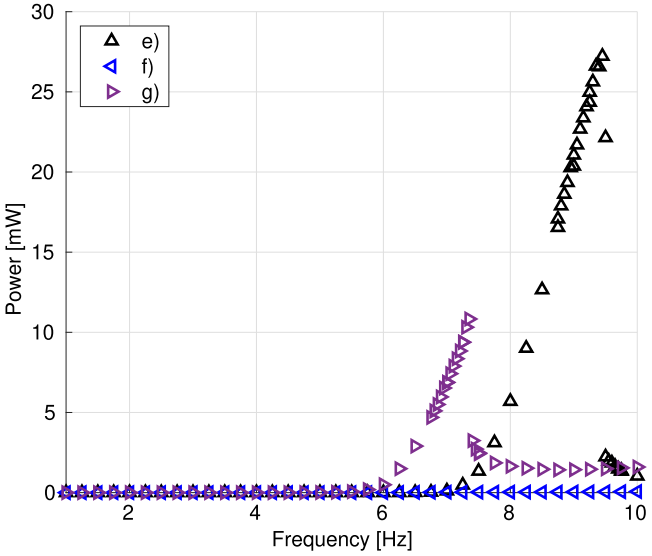

Fig. 7. The power as function of frequency in the x-direction for the device configurations given in Table 3. The y-direction has a fixed frequency of 4 Hz.

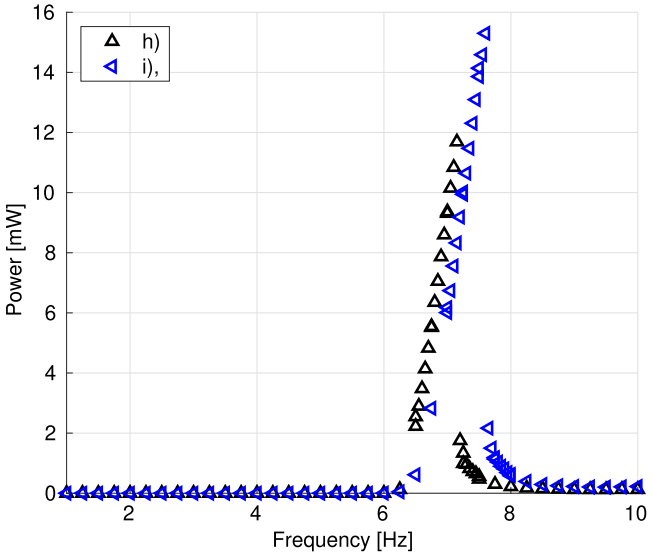

Fig. 8. The power as function of frequency in the x-direction for the device configurations given in Table 4. The y-direction has a fixed frequency of 4 Hz.

4.4. Electromagnetic damping

Besides the magnetic stiffness in the harvester, the electromagnetic damping provided by the coils will also affect the movement of the free magnet and therefore the power output of the device. To investigate this effect, the "e"-case harvester is taken which was able to scavenge the highest power compared to the other configurations. For this system two different coil windings are employed, with different dimensions and different number of turns. Table 5 shows the characteristics of two new coils. Both use the original "e"-case coils as reference, see Table 1, but one coil has an increased diameter, whereas the other has an increased thickness. For both coils the number of turns is increased to 500 turns to accommodate the larger dimensions. This also increases the total wire length and increases the internal electrical resistance to 60 Ω and 68 Ω respectively. The load resistance in the experiments was changed according, i.e. to match the coil internal resistance. Performing the same vibrational experiments as described

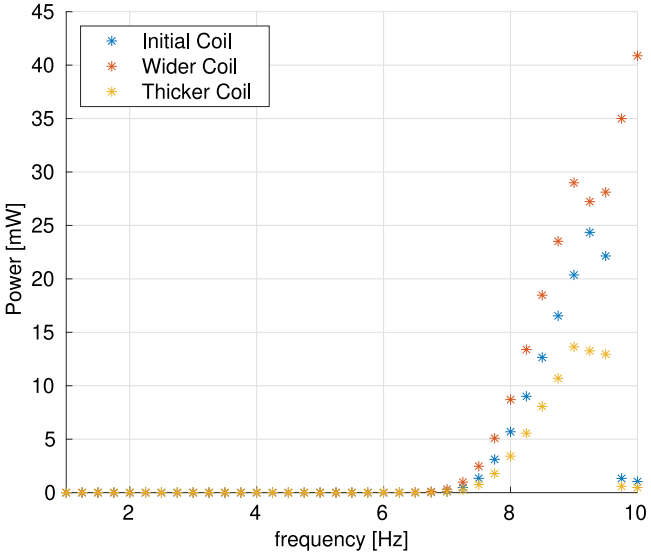

Fig. 9. Power as function of frequency for configuration "e" with three different coils.

Table 5
The parameters for the different coils tested.

Coils	Parameter	Quantity
Wider	Inner diameter	27 mm
	Outer diameter	51 mm
	Height	2.5 mm
	Number of turns	500
	Wire gauge	0.202 mm
	Resistance	60 Ω
	Inductance	11.5 mH
Thicker	Inner diameter	27 mm
	Outer diamter	40 mm
	Height	5 mm
	Number of turns	500
	Wire gauge	0.202 mm
	Resistance	68 Ω
	Inductance	10.3 mH

previously, i.e. a frequency sweep in one direction while maintaining a 4 Hz vibration in the other direction, the power produced by the harvester with the different coils mounted was measured. The results are shown in Fig. 9 where it can be seen that the different coils modify the state of the system, attaining a different resonance frequency as by modifying the magnetic stiffness. Moreover, it is seen that the wider coil clearly produces more power compared to the initial and thicker coils. The reason for this is that the thicker coil brings about a larger air-gap between the moving magnet and the coil-loops at one end of the coil. Consequently, lower voltage is induced on those coil-loops, and its higher internal resistance limits the electrical current, given as a result a lower output power compared with the other two coil windings.

4.5. Two dimensional frequency sweep

Until now, all experiments have been performed with a varying frequency in one direction and a 4 Hz vibration in the other direction. To explore the influence of the previously fixed 4 Hz frequency, the best performing device, i.e. "e"-case with a wider coil, was experimentally characterized with a frequency sweep study in both directions. The experimental procedure remains the same as previously described, i.e. for each pair of frequencies the system is started from rest and the steady state properties of the system is measured. The results are shown in Fig. 10 where it can be seen that the harvester has a fairly broad band with a width of around 6 Hz in the y-axis frequency centered on 3 Hz.

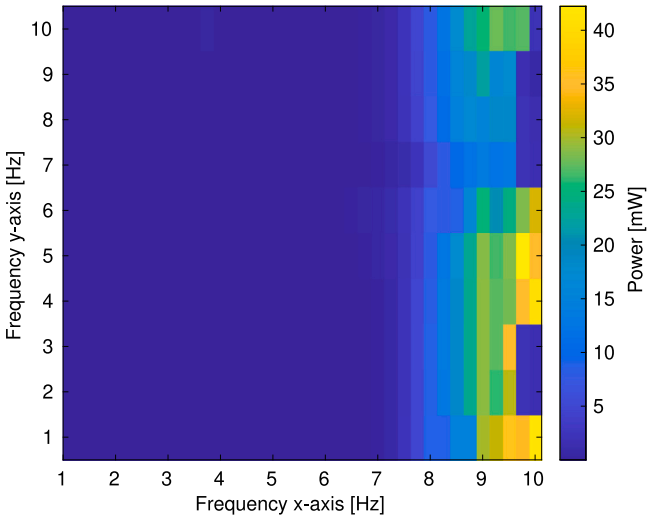

Fig. 10. Output power of the harvester with wider coil windings.

Compared to a previously constructed ellipsoidal two-dimensional electromagnetic vibrational harvester [19], the harvester investigated in this work has a boarder frequency span in the *y*-axis, which is likely due to the low magnetic stiffness in this direction for the particular harvester investigated here, i.e. the "e"-case .

4.6. Discussion

The above experiments have revealed a number of facts that is of interest when designing future harvesters. The most interesting of these is that breaking the symmetry of the restoring force internally in the harvester means that the free-to-move structure can move in a way that generates a factor of two more power for the size of device considered here. Furthermore, not only is the power increased, the frequency range at which the harvester generates useful power is also significantly increased.

One thing that has not been explored in this work is the hysteresis behavior, which electromagnetic harvesters are known to display [9,18,32,33]. This hysteresis behavior is a consequence of the fact that the systems has multiple stable solutions in the device phase space [33–36]. For the harvester characterized in this work, the harvester for each frequency tested is started from rest. If the harvester had been taken through a different frequency history to reach the operated frequency, e.g. by reaching the operating frequency by decreasing from a higher frequency, a different energy state with a different power might be reached. The 2D shaker used in this work did not allow for this experiment, so this should be explored in a future study.

5. Conclusion

In this work a novel two-dimensional electromagnetic vibration energy harvester has been introduced and experimentally characterized by subjecting it to two-dimensional vibrations. The magnetic stiffness in the harvester has been varied by distributing the permanent magnets in the ring structure of the harvester in nine different configurations. Additionally, the electromagnetic damping created by the magnet–coil interaction has been compared for three different coil windings. The experimental results showed that the more magnets in the ring structure, the stronger restoring force and the higher the resonance frequency of the harvester. Furthermore, by concentrating the number of magnets on one motion axis, making the harvester asymmetric, the harvester resonance frequency increases slightly but the output power increases to twice as large a value as the symmetric configurations. In addition, it was shown that choosing the proper coil dimensions can lead to a larger power, but that this will also slightly increase resonance frequency of the harvester. The largest power output of the harvester was 42 mW, representing a good alternative as energy supply for the booming market of low-power devices.

CRediT authorship contribution statement

Carlos Imbaquingo: Writing – original draft, Software, Experimental work. **Christian Bahl:** Conceptualization, Writing. **Andrea R. Insinga:** Conceptualization, Writing. **Rasmus Bjørk:** Conceptualization, Data curation, Software, Writing.

Declaration of competing interest

The authors declare that they have no known competing financial interests or personal relationships that could have appeared to influence the work reported in this paper.

Data availability

Data presented in this work is directly available from Ref. [37].

Acknowledgments

The authors wish to thank the Independent Research Fund Denmark, project 8022-00038B for sponsoring this work. The authors wish to thank Philip Holm for assisting in performing the electromagnetic damping experiments.

References

[1] Ahmad Iftikhar, Meng Lim, Abdelrhman Ahmed M, Asad Syed, Leong MS. Scopes , challenges and approaches of energy harvesting for wireless sensor nodes in machine condition monitoring systems : A review. Measurement 2021;183(April):109856.
[2] Ahmed Majd S. Designing of internet of things for real time system. Mater Today: Proc 2021.
[3] Priya Shashank, Inman Daniel J. Energy harvesting technologies. Springer US; 2009, p. 1–517.
[4] Melchor-Martínez Elda M, Macias-Garbett Rodrigo, Malacara-Becerra Alonso, Iqbal Hafiz MN, Sosa-Hernández Juan Eduardo, Parra-Saldívar Roberto. Environmental impact of emerging contaminants from battery waste: A mini review. Case Stud Chem Environ Eng 2021;3(November 2020):100104.
[5] Von Büren Thomas, Lukowicz Paul, Tröster Gerhard. Kinetic energy powered computing - an experimental feasibility study. In: Proceedings - international symposium on wearable computers. 2003, p. 22–5.
[6] Cepnik Clemens, Lausecker Roland, Wallrabe Ulrike. Review on electrodynamic energy harvesters - a classification approach. Micromachines 2013;4:168–96.
[7] Blokhina Elena, Aroudi El. Nonlinearity in energy harvesting systems. Springer International Publishing; 2016.
[8] Jensen Tobias Willemoes, Insinga Andrea R, Ehlers Johan Christian, Bjørk Rasmus. The full phase space dynamics of a magnetically levitated electromagnetic vibration harvester. Sci Rep 2021;11(1):1–15.
[9] Mann BP, Sims ND. Energy harvesting from the nonlinear oscillations of magnetic levitation. J Sound Vib 2009;319(1–2):515–30.
[10] Morais Raul, Silva Nuno M, Santos Paulo M, Frias Clara M, Ferreira Jorge AF, Ramos Antonio M, et al. Double permanent magnet vibration power generator for smart hip prosthesis. Sensors Actuators A 2011;172(1):259–68, Eurosensors XXIV, Linz, Austria, 5-8 September 2010.
[11] Dos Santos Marco P Soares, Ferreira Jorge AF, Simões José AO, Pascoal Ricardo, Torrão João, Xue Xiaozheng, et al. Magnetic levitation-based electromagnetic energy harvesting: A semi-analytical non-linear model for energy transduction. Sci Rep 2016;6(1):1–9.
[12] Imbaquingo Carlos Enrique, Beleggia Marco, Insinga Andrea Roberto, Bahl Christian RH, Mann Brian, Bjørk Rasmus. Analytical force and flux for a 1-D electromagnetic vibration energy harvester. IEEE Trans Magn 2020;56(11):1–6.
[13] Cheng Shuo, Wang Naigang, Arnold David P. Modeling of magnetic vibrational energy harvesters using equivalent circuit representations. J Micromech Microeng 2007;17(11):2328.
[14] Wang Yifeng, Li Shoutai, Gao Mingyuan, Ouyang Huajiang, He Qing, Wang Ping. Analysis, design and testing of a rolling magnet harvester with diametrical magnetization for train vibration. Appl Energy 2021;300:117373.

[15] Sato Takahiro, Igarashi Hajime. A chaotic vibration energy harvester using magnetic material. Smart Mater Struct 2015;24(2):025033.
[16] Choi Yunhee, Ju Suna, Chae Song Hee, Jun Sangbeom, Ji Chang-Hyeon. Low-frequency vibration energy harvester using a spherical permanent magnet with controlled mass distribution. Smart Mater Struct 2015;24(6):065029.
[17] Carneiro Pedro, dos Santos Marco P Soares, Rodrigues André, Ferreira Jorge A F, Simões José AO, Marques A Torres, et al. Electromagnetic energy harvesting using magnetic levitation architectures: A review. Appl Energy 2020;260:114191.
[18] Nguyen Hieu Tri, Genov Dentcho A, Bardaweel Hamzeh. Vibration energy harvesting using magnetic spring based nonlinear oscillators: Design strategies and insights. Appl Energy 2020;269:115102.
[19] Imbaquingo Carlos, Bahl Christian, Insinga Andrea R, Bjørk Rasmus. Two-dimensional elliptically shaped electromagnetic vibration energy harvester. 2022, [submitted for publication, arXiv].
[20] Gutierrez Manuel, Shahidi Amir, Berdy David, Peroulis Dimitrios. Design and characterization of a low frequency 2-dimensional magnetic levitation kinetic energy harvester. Sensors Actuators A 2015;236:1–10.
[21] Bowers Benjamin J, Arnold David P. Spherical, rolling magnet generators for passive energy harvesting from human motion. J Micromech Microeng 2009;19(9).
[22] Sasaki Ken, Osaki Yuji, Okazaki Jun, Hosaka Hiroshi, Itao Kiyoshi. Vibration-based automatic power-generation system. Microsyst Technol 2005;11(8–10).
[23] Fitzgerald Arthur Eugene, Kingsley Charles, Umans Stephen D. Electric machinery. McGraw-Hill; 2003, p. 688 s..
[24] Kecik Krzysztof, Kowalczuk Marcin. Effect of nonlinear electromechanical coupling in magnetic levitation energy harvester. Energies 2021;14(9):2715.
[25] Saha CR, O'donnell T, Wang N, McCloskey P. Electromagnetic generator for harvesting energy from human motion. Sensors Actuators A 2008;147(1):248–53.
[26] Liu Huicong, Gudla Sudeep, Hassani Faezeh Arab, Heng Chun Huat, Lian Yong, Lee Chengkuo. Investigation of the nonlinear electromagnetic energy harvesters from hand shaking. IEEE Sens J 2014;15(4):2356–64.
[27] Zhang Qian, Wang Yufeng, Kim Eun Sok. Power generation from human body motion through magnet and coil arrays with magnetic spring. J Appl Phys 2014;115(6):064908.
[28] Berdy DF, Valentino DJ, Peroulis D. Kinetic energy harvesting from human walking and running using a magnetic levitation energy harvester. Sensors Actuators A 2015;222:262–71.
[29] Geisler Matthias, Boisseau Sebastien, Perez Matthias, Gasnier Pierre, Willemin Jerome, Ait-Ali Imene, et al. Human-motion energy harvester for autonomous body area sensors. Smart Mater Struct 2017;26(3):035028.
[30] Wang Wei, Cao Junyi, Zhang Nan, Lin Jing, Liao Wei-Hsin. Magnetic-spring based energy harvesting from human motions: design, modeling and experiments. Energy Convers Manage 2017;132:189–97.
[31] Struwig Michael N, Wolhuter Riaan, Niesler Thomas. Nonlinear model and optimization method for a single-axis linear-motion energy harvester for footstep excitation. Smart Mater Struct 2018;27(12):125007.
[32] Wang Wei, Wei Hongtao, Wei Zon-Han. Numerical analysis of a magnetic-spring-based piecewise nonlinear electromagnetic energy harvester. Eur Phys J Plus 2022;137(1):56.
[33] Carneiro Pedro MR, Vidal João V, Rolo Pedro, Peres Inês, Ferreira Jorge AF, Kholkin Andrei L, et al. Instrumented electromagnetic generator: Optimized performance by automatic self-adaptation of the generator structure. Mech Syst Signal Process 2022;171:108898.
[34] Kecik Krzysztof, Mitura Andrzej, Lenci Stefano, Warminski Jerzy. Energy harvesting from a magnetic levitation system. Int J Non-Linear Mech 2017;94:200–6.
[35] Kecik Krzysztof. Energy recovery from a non-linear electromagnetic system. Acta Mech Automat 2018;12(1).
[36] Jensen Tobias Willemoes, Insinga Andrea R, Ehlers Johan Christian, Bjørk Rasmus. The full phase space dynamics of a magnetically levitated electromagnetic vibration harvester. Sci Rep 2021;11(1):16607.
[37] Imbaquingo Carlos, Bahl Christian, Insinga Andrea R, Bjørk Rasmus. Data set for "a two-dimensional electromagnetic vibration energy harvester with variable stiffness". Data.dtu.dk 2022.